Fracture Mechanics of Concrete Structures
Proceedings FRAMCOS-3
AEDIFICATIO Publishers, D-79104 Freiburg, Germany

FRACTURE ANALYSIS OF STEEL PLATE ANCHORS IN CONCRETE BY USING RBSM

H. Kitoh
Research Associate, Dept. of Civil Engrg., Osaka City Univ., Japan
N. Takeuchi
Professor, Dept. of Civil Engrg., Meisei Univ., Japan
M. Ueda and A. Kambayashi
Head and Researcher, Research & Development Inst., Takenaka Co., Japan
H. Higuchi
Head, Dept. of Information System, Abe Co., Japan
M. Tomida
Lecturer, Dept. of Civil Engrg., Ishikawa Nat'l College of Tech., Japan

Abstract
Rigid Bodies-Spring Model, abbreviated to RBSM, has been developed as a computational model generalizing limit analysis in plasticity, in which a structure to be analyzed is idealized as an assemblage of rigid bodies connected by normal and tangential springs. Thus, RBSM is so useful for fracture analysis of concrete cracking, which can be regarded as a well-known discrete crack model. In this paper, we present two numerical examples of fracture analysis of concrete cracking due to a steel plate anchor; One is a pull-out test of the T-shaped anchor, and the other is a direct shear test of the I-shaped anchor, which is called a shear connector in composite construction.
Key words: cracking of concrete, anchor, Rigid Bodies-Spring Model

1 Introduction

A family of Rigid Bodies-Spring Model, abbreviated to RBSM, has been developed by Kawai (1977) as a computational model generalizing limit analysis in plasticity, based on the experimental evidence of solids under the ultimate state of loading. In those modelling, the solid or structure to be analyzed is idealized as an assemblage of rigid bodies connected each other on their interfaces by normal and tangential springs introduced the mechani-

cal properties. Thus, RBSM is so useful in essence for the analysis including the discontinuous behavior such as separation that it can also be applied sufficiently to the fracture analysis of concrete structures with discontinuity due to cracking and slippage in concrete.

Therefore, introducing a strain softening curve dependant upon the concept of fracture energy, we, Kitoh et al. (1997), have applied RBSM to a size effect analysis of concrete beams without reinforcement, and then have obtained the successful results.

In this paper, we present the following two numerical examples by using RBSM, where the fracture of concrete such as tensile cracking and shear slippage can play an intensive role in the nonlinear behaviors of concrete structures: First, a pull-out test of T-shaped steel plate anchor bolts was analyzed, the test which is analogous to that of RILEM TC-90 FMA reported by Elfgren (1991). Second, we also carried out the analysis of a direct shear problem of I-shaped steel plate anchors, those are commonly called shear connectors in steel-concrete composite construction. In this second example, the anchor was subjected to a horizontal load with respect to its longitudinal axis, while the load was applied in the same direction of the axis of the anchor in the first example.

2 Formulation of a Two Dimensional RBSM

We considered two rigid triangular elements as shown in Fig. 1. An arbitrary polygon of circle, of course, can be used instead of a triangular element. They are assumed to be in equilibrium with external loads and reaction force of the spring system which are distributed over the contact surface of two adjacent elements.

The rigid displacement field is assumed in each element in terms of the displacement (u, v, θ) of the centroid as shown in Fig. 1. More precisely horizontal and vertical displacement U, V at the arbitrary point P can be given by the following equations:

$$\boldsymbol{U} = \boldsymbol{Q} \cdot \boldsymbol{u} \tag{1}$$

$$U = \{U_I,\ V_I,\ U_{II},\ V_{II}\}^T$$

$$u = \{u_1,\ v_1,\ \theta_1,\ u_2,\ v_2,\ \theta_2\}^T$$

$$Q = \begin{pmatrix} 1 & 0 & -(y-y_1) & 0 & 0 & 0 \\ 0 & 1 & (x-x_1) & 0 & 0 & 0 \\ 0 & 0 & 0 & 1 & 0 & -(y-y_2) \\ 0 & 0 & 0 & 0 & 1 & (x-x_2) \end{pmatrix}$$

where subscript I, II or 1, 2 indicate element number 1 or 2, respectively. (x_1, y_1) and (x_2, y_2) are the coordinate values of the centroid of each element.

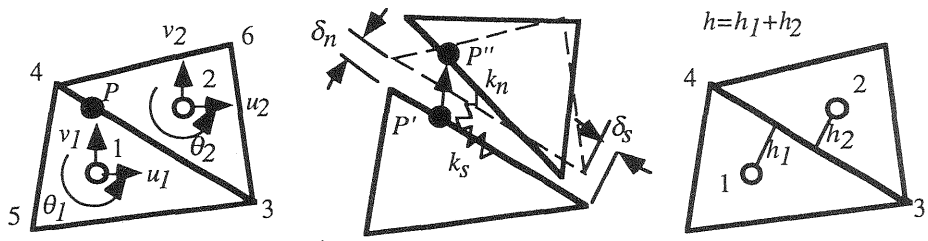

(a) Degree of freedom (b) Deformed state (c) Projective length

Fig.1 Two dimensional rigid triangular elements

The relation of the displacement between the global coordinate system and the local one along side 34 of the element is derived as follows:

$$\overline{U} = \boldsymbol{R} \cdot \boldsymbol{U} \tag{2}$$

$$\overline{U} = \left\{ \overline{U_I},\ \overline{V_I},\ \overline{U_{II}},\ \overline{V_{II}} \right\}^T : \boldsymbol{R} = \begin{pmatrix} l_1 & m_1 & 0 & 0 \\ l_2 & m_2 & 0 & 0 \\ 0 & 0 & l_1 & m_1 \\ 0 & 0 & l_2 & m_2 \end{pmatrix} : \begin{matrix} l_1 = \cos(\overline{x}, x) = y_{43} / l_{34} \\ l_2 = \cos(\overline{x}, y) = x_{43} / l_{34} \\ m_1 = \cos(\overline{y}, x) = x_{34} / l_{34} \\ m_2 = \cos(\overline{y}, y) = y_{34} / l_{34} \end{matrix}$$

where l_{34} is the length of the side 34, $x_{ij}=x_i-x_j$, the overbar indicates the local coordinate system and $\boldsymbol{R}$ is a coordinate transformation matrix.

Using these displacements ($\overline{U}$, $\overline{V}$) with the local coordinate system, the relative displacement vector δ of the point P can be derived as follows:

$$\delta = \boldsymbol{M} \cdot \overline{\boldsymbol{U}} \tag{3}$$

$$\delta = \{ \delta_n,\ \delta_s \}^T : \boldsymbol{M} = \begin{pmatrix} -1 & 0 & 1 & 0 \\ 0 & -1 & 0 & 1 \end{pmatrix}$$

Therefore, substituting Eq. (1) and Eq. (2) into Eq. (3), the following relation with the rigid displacement field is easily obtained:

$$\delta = \boldsymbol{M} \cdot \boldsymbol{R} \cdot \boldsymbol{Q} \cdot \boldsymbol{u} = \boldsymbol{B} \cdot \boldsymbol{u} \tag{4}$$

The stress - relative displacement relation in plane stress condition is assumed as follows:

$$\sigma = \boldsymbol{D} \cdot \delta \tag{5}$$

$$\sigma = \{ \sigma_n,\ \tau_s \}^T : \boldsymbol{D} = \begin{pmatrix} k_n & 0 \\ 0 & k_s \end{pmatrix} : k_n = \frac{(1-\nu)E}{(1-2\nu)(1+\nu)h} \ :\ k_s = \frac{E}{(1+\nu)h}$$

where k_n and k_s are the spring constant which resist normal and tangential forces respectively on the contact surface between element 1 and element 2.

Furthermore $h=h_1+h_2$ is the projected length of a vector connecting centroids along the line perpendicular to 34, as shown in Fig. 1(c)

On the other hand, strain components are determined by using the finite difference equation as follows:

$$\varepsilon=\begin{pmatrix}\varepsilon_n\\ \gamma_s\end{pmatrix}=\frac{1}{h_1+h_2}\begin{pmatrix}\delta_n\\ \delta_s\end{pmatrix}=\frac{1}{h}\delta \tag{6}$$

Based on the above preliminaries, the strain energy expression of the in-plain element V can be obtained as the following matrix equation:

$$V=\frac{1}{2}\int_{l_{34}}\delta^T\cdot\boldsymbol{D}\cdot\delta ds=\frac{1}{2}\boldsymbol{u}^T\int_{l_{34}}(\boldsymbol{B}^T\cdot\boldsymbol{D}\cdot\boldsymbol{B})ds\cdot\boldsymbol{u} \tag{7}$$

Applying Castigliano's theorem to Eq. (7) the following stiffness equation can be derived:

$$\frac{\partial V}{\partial \boldsymbol{u}}=\boldsymbol{K}\cdot\boldsymbol{u}=\boldsymbol{P} \tag{8}$$

where $\boldsymbol{K}$ is a (6 x 6) symmetric matrix and $\boldsymbol{P}$ is a nodal load vector corresponding to the displacement vector $\boldsymbol{u}$ in Eq. (1) defined as follows:

$$\boldsymbol{P}=\{X_1,\ Y_1,\ M_1,\ X_2,\ Y_2,\ M_2\}^T \tag{9}$$

3 Constitutive Law of Concrete

The broken line on Fig. 2 shows the uniaxial stress - strain curve of the concrete. In the numerical calculations, this curved line is approximated according to the trilinear solid line. In this paper, F_c being the compressive strength, the first yield level $F_{c1}=0.5F_c$, the second yield level $F_{c2}=0.95F_c$, and the reduction ratio of the stiffness $\beta=0.5$. After the second yielding at ε_{cu} (0.3%), F_{c2} is maintained until collapse. Beyond this point, until reaching $2\varepsilon_{cu}$, the stress decreases with a corresponding increase in the strain, and it stays finally at $0.2F_c$. The strain softening effect is thereby taken into consideration. The tensile stress is released going along the linear function connecting with $(F_t,\ \varepsilon_{cr})$ and $(0,\ n\varepsilon_{cr})$ is introduced where n can be determined by fracture energy G_F, for instance, which is given as used by Rots (1992):

$$G_F=\frac{1}{2}h\cdot F_t(n-1)\varepsilon_{cr}\ \Rightarrow\ n=\frac{2G_F}{h\cdot F_t\cdot\varepsilon_{cr}}+1 \tag{10}$$

where h is the projective length as shown in Fig. 1(c), which is a representative index of the element size in RBSM.

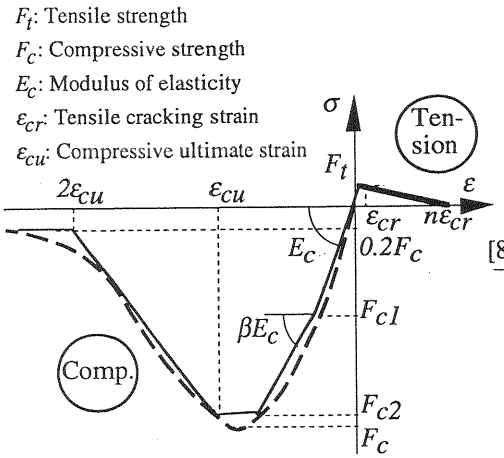

Fig.2 Stress - strain relation for concrete

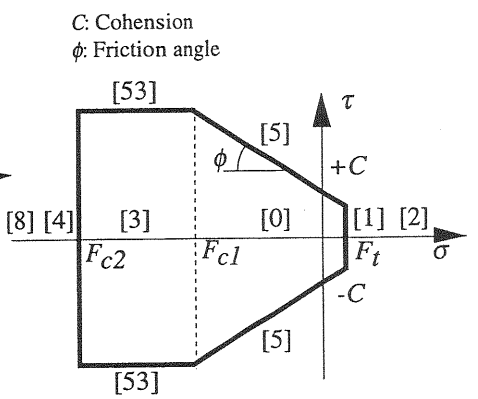

Fig.3 Yield and collapse surface for concrete

The shearing slippage surface is defined by Mohr - Coulomb's criterion, and after yielding, the associate flow rule is employed, and moves in the surface. Based on the supposition above, Fig. 3 shows the yield and collapse surface of concrete using RBSM. The state [0] shows elasticity, the surface [1] is cracking, the state [2] is the condition where the residual stresses become zero, in Fig. 3, that is a state of tension on the left side from $n\varepsilon_{cr}$. The state [3] shows first yield, the surface [4] shows second yield, and the state [8] is the normal strain having the condition reached at the strain limit of Fig. 3. The surface [5] shows shear slippage. After this state, in case where first yield compression of the state [3] has occurred, the state follows the stage in the surface [53]

4 Nonlinear Analysis Algorithm

In concrete structures, shapes change as cracking develops, and then stress is released on the cracking surface. The released stress or load leads to a decline of convergence of solutions near and at the ultimate stage of loading. To overcome this condition, Kawai et al. (1990), including some of us, proposed an algorithm for material nonlinear analysis, in which r_{min} method by Yamada et al. (1968) was modified to add the released force to the remaining load while counting the applied load, and to simultaneously take account of the slip, cracking and compressive failure.

However, the algorithm is to be originally applied to an incremental load method. This method is inadequate to simulate the crack propagation in detail, because the cracking failure of concrete is brittle. The algorithm can

Table 1 Details of the pull-out specimens

Tag	Size(mm)				Spring	Concrete Properties						
	d	a	b	L	K	F_c (MPa)	F_t (MPa)	E_c (GPa)	G_F (N/m)	C^* (MPa)	ϕ^* (°)	v^*
#1	150	300	100	900	0	30.0	3.0	30.0	100	4.14	37.0	.167
#2	60	60	80	350	∞	34.3	3.4	29.4	100	4.68	37.0	.167

Note: * prescribed by ourselves, while the others were given by JCI(1993)

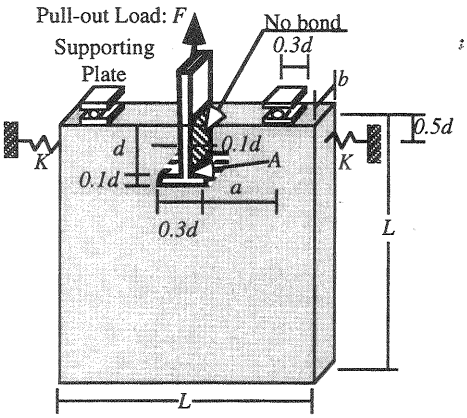

Fig. 4 Pull-out specimen

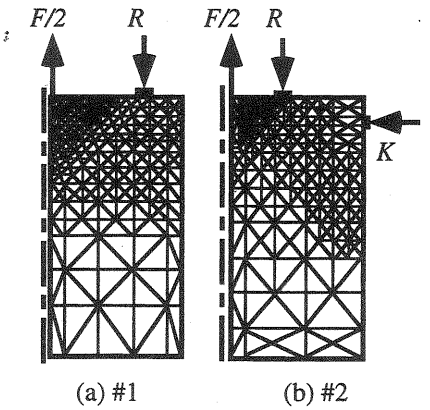

Fig. 5 Mesh used in the analysis

also be applied to an incremental displacement method if the incremental displacement is taken and external force. Thus, the following nonlinear analysis was carried out to an incremental displacement method.

5 Pull-out Test of T-shaped Steel Plate Anchor in Concrete

In the first example, the 2 tests to be analyzed were given as the Round Robin Tests by JCI (1993). The details of two specimens are shown in Table 1 and Fig. 4. As for steel, material properties used were as follows: Modulus of elasticity, Poisson's ratio and yield point were 210 GPa, 0.3 and 400 MPa, respectively. Furthermore, the meshes used are also shown in Fig. 5, those are half regions of the specimens considering symmetry. As shown in Fig. 4, a T-shaped steel plate anchor embedded in a concrete block was subjected to pull-out force along its longitudinal axis, and the block was vertically supported by 2 stiff steel plates on parts of its top surface and also laterally supported by 2 springs, those constants were K, on both of its side surface.

Figure 6 a) shows the obtained relation on #1 specimen between the non-dimensional pull-out force and the upward displacement of the anchor at

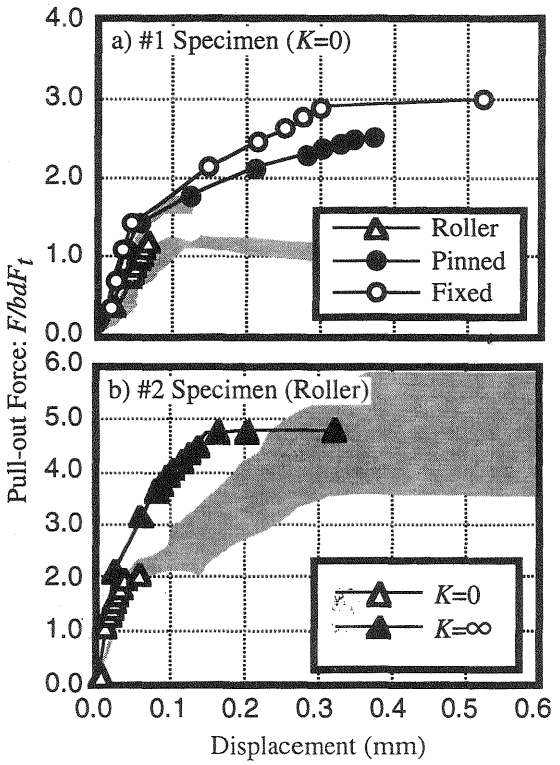

Fig. 6 Load - displacement relation

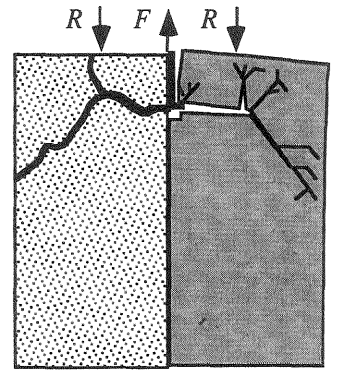

Fig. 7 Crack pattern
(#2; K=0; Roller)

point A as shown in Fig. 4. Shaded regions in the figure indicate the experimental results by JCI (1993). We adopted 3 vertical support conditions, those were roller, pinned or fixed one. The influence of the support condition upon the obtained solution was significant. Therefore, the solution with roller supports was close to a lower band of the experimental results, while that with pinned supports was close to a upper bound of them.

Next, Fig, 6 b) shows the obtained relation on #2 specimen as same as Fig. 6 a). We adopted 2 lateral spring constants; One was zero, and the other was infinity. As same as the above example, the influence of the lateral support condition upon the solution was also pronounced. Thus the solution with rigid lateral supports fairly agreed with the experimental results, whose load carrying capacity was 2.5 times large as that without lateral supports.

Last, Fig. 7 compares cracking patterns obtained from the analysis and an experiment by ourselves. It can be seen that the numerical result was sufficiently trace the experimental one. Moreover, the steel plate almost never deformed, while the deformation of concrete due to cracking was remarkable as shown in the figure.

Table 2 Material Properties

Concrete							Steel Plate for beam elements*					
F_c (MPa)	F_t (MPa)	E_c (GPa)	G_F (N/m)	C (MPa)	ϕ (°)	ν	E_b (GPa)	G_b (GPa)	A_b (cm²)	I_b (cm⁴)	N_{by} (kN)	M_{by} (kNm)
45.1	3.76	32.2	100	6.23	37.0	0.20	210	81.0	22.0	1.45	869	19.3
							ditto.	ditto.	14.3	0.39	561	8.12

Notes: E_b,G_b,A_b,I_b,N_{by} and M_{by} are Elastic modulus, Shear rigidity, Cross sectional area, Moment of inertia, Yielding axial force and Yielding moment, respectively.
*Top numerals for the base plate, while bottom ones for the anchor.

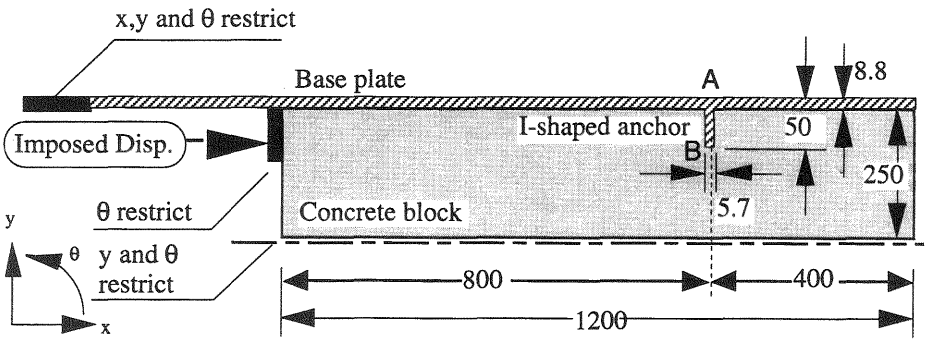

Fig. 8 Direct shear specimen (unit: mm; depth 250)

6 Direct Shear Test of I-shaped Steel Plate Anchor in Concrete

In the second example, the tests to be analyzed were carried out by Nippon Steel Co. (1993) as a fundamental work for the design of a steel plate - concrete composite immersed tunnel having 6 lanes of roadway and 520 m in total length, now under construction in Japan. The outline of a specimen is shown in Fig. 8, where a half region of the specimen is drawn considering symmetry. Furthermore, the material properties are listed in Table 2. Moreover, the steel material properties used were same as those in the previous example.

As shown in Fig. 8, a I-shaped steel plate anchor embedded in a concrete block was subjected to lateral force due to pull-out action of a base plate. Thus, the base plate had no restriction for out-plane deformation and the anchor plate was under bending moment and shear force. In this example, therefore, we alternatively attended to use beam elements instead of 2 dimensional elements for the steel plates' part, since the plates were so thin that their out-plane deformation mainly due to bending could be expected not to be negligible. The mechanical properties of the beam element is also listed in Table 2.

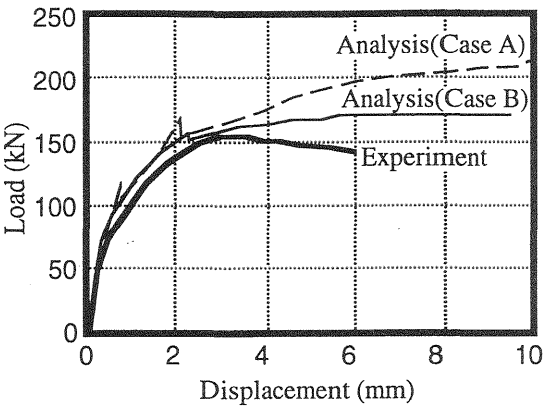

Fig.9 Load - displacement relation

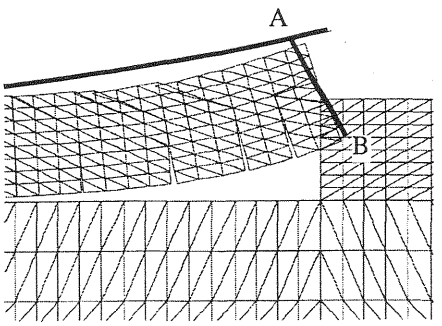

Fig.10 Crack Pattern
(Numerical; Case B)

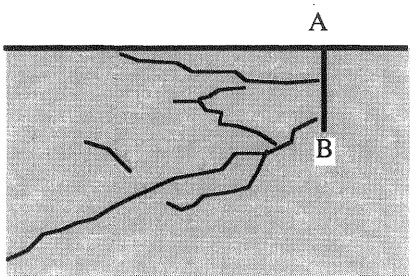

Fig.11 Crack Pattern
(Experimental)

Figure 9 shows the load due to the imposed displacement - leftward displacement at the point A in Fig. 8 relations obtained from the analyses and the experiment. From the figure, it can be seen that the solution from the analysis where the beam elements were used for the steel plate, called case B hereafter, was more flexible and closer to the experiment result than the another solution where 2 dimensional element were used for the plate, called case A hereafter. This difference could be caused by the deformation of the plate in case B to reduce the shear resistance of the anchor.

Next, the failure mode near the anchor obtain from the solution of case B are shown in Fig. 10. In this figure, separating elements shows cracking , while overlapping ones does crushing which indicates a bearing failure in front of the anchor observed in the experiment. While the mode from the experiment are shown in Fig. 11. Comparing between the figures, the solution could fairly trace the experimental result.

7 Concluding Remarks

RBSM, introducing the concept of fracture energy, has successfully simulated the brittle behavior due to concrete cracking through the two numerical examples demonstrated herein. Thus, we could verified the applicability of RBSM to fracture analysis of concrete structures.

8 References

Elfgren, L. (1991) Round-robin analysis of anchor bolts, RILEM TC-90 FMA, **Fracture Mechanics of Concrete - Application**, Preliminary report

JCI (1993) **Applications of Fracture Mechanics to Concrete Structure** (ed. H. Mihashi), (in Japanese)

Kawai, T. (1977) New element models in discrete structural analysis, **Journal of the Society of Naval Architectures of Japan**, 141, 187-193

Kawai, T. et al. (1990) Application of discrete limit analysis to reinforced concrete shear panel, in **Proceedings of the Second World Congress on Computational Mechanics**, Stuttgart, F.R.G., 862-865

Kitoh, H., Takeuchi, N., Ueda, M., Higuchi, H., Kambayashi, A. and Tomida, M. (1997) Size effect analysis of plain concrete beams by using RBSM, in **Proceedings of the Second International Conference on Analysis of Discontinuous Deformation** (ed. Y. Ohnishi), Kyoto, Japan, 373-382

Nippon Steel Corporation (1993) **Report on the load carrying capacity tests of various shaped steel plate shear connectors with no restriction against out-plane deformation of base plate**, 1-32 (in Japanese)

Rots, J.G. (1992) Removal of finite elements in strain - softening analysis of tensile fracture, in **Fracture Mechanics of Concrete Structures**, (ed. Z. P. Bazant), Elsevier Applied Science, 330-338

Yamada, Y., Yoshimura, N. and Sakurai, T. (1968) Plastic stress - strain matrix and its application for the solution of elasto-plastic problem by a finite element method, **International Journal of Mechanical Science**, 10, 343-354